Walking Control Algorithm based on Polynomial Trajectory Generation

MARCO PEREZ-CISNEROS * **ERIK CUEVAS** ** **DANIEL ZALDIVAR** **

* *CUCEI, Universidad de Guadalajara, Av. Revolucion 1500,C.P. 44430 Guadalajara, Jal., Mexico (Tel: +52 33 13785900 Ext 7731; e-mail: marcopc@cucei.udg.mx).*
** *Institut für Informatik, Freie Universität Berlin Takustr. 9, 14195 Berlin, Germany, (e-mail: cuevas@mi.fu-berlin.de, zaldivar@mi.fu-berlin.de)*

Abstract: Humanoid walking trajectory is a complex task, due the high number of degrees of freedom (DOFs) and changes on the mechanical structure during walking. A non-trivial problem in bipedal robot walking is the instability produced by violent transitions between different walk phases. This work presents a trajectory generation algorithm for a biped robot. The algorithm is based on cubic Hermitian polynomial interpolation of the initial conditions of the robot. This algorithm guarantees a smooth transition in the walking phases reducing significantly the tendency for falling down when the walking speed increases or the terrain conditions changes. The algorithm was successfully tested on the biped robot "Dany walker", which was designed at the Freie Universität Berlin, Germany and the University of Guadalajara, México.

1. INTRODUCTION

Robots have to be able to adapt to complicated environments, such as rugged terrain, sloped surfaces, and steep stairs. Biped robots can walk in almost any type of terrain, including those which are impossible for wheeled robots as in Goddard [1992], Kanehira [2002] and Konno [2000]. However, biped robots, which are complex nonlinear systems with many degrees of freedom, can fall down easily while walking due to its relatively small feet. Extensive researches have been conducted on bipedal walking, and now biped robots are capable of walking with a certain amount of stability. Yet, these biped robots still show a tendency for falling down as walking speed increases or when the terrain conditions changes.

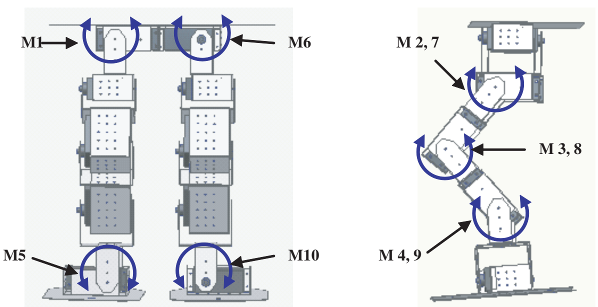

(a) (b)

Fig. 1. "Dany Walker" biped robot, motor location: (a): Frontal plane. (b): Saggital plane.

In this paper, we propose a simple and effective walking trajectory method based on cubic Hermitian polynomial interpolation of the kinematics positions of the robot. A Hermite spline is a cubic polynomial interpolation in segments with adjustable derivatives at each control point. This is an important property for the generation of robot's trajectories, since it allows diminishing the link velocities while arriving to the final point, reducing the characteristic impact on the leg as soon as it establishes ground contact. The walking trajectory is generated for each joint, adjusting some intermediate positions that assure a correct zero moment point (ZMP) trajectory. Because the ZMP trajectory is mainly determined by the trajectory of the center of gravity (CoG), it is possible to reduce the ZMP error by simply modifying the position of the CoG in some points during walking. Polynomial Trajectory Algorithm (PTA) has several advantages compared to other methods. PTA is simple, so it is suitable for generating trajectories for bipedal walking in real time. If it can be generated in real time, a robot might not fall down even if it is walking on uneven ground or the walking speed changes.

This paper is organized as follows: Section 2 introduces a biped robot model and walking motion for bipedal walking. Section 3 describes PTA and the important parameters. In Section 4, we obtain the walking motions which are generated by the polynomial trajectory algorithm and compared against other methods when changing the terrain type. Finally, conclusions follow in Section 5.

2. ROBOT MODEL AND WALKING METHOD

2.1 Robot model

The dynamics of a biped robot is closely related to its structure as explained in Cuevas [04] by means of the "Dany Walker" robot, which has been built using 10 low-density aluminum links. Each link consists of a structure which has been carefully designed to allow an effective torque transmission and low deformation. All links are connected building a biped robot of 10 degrees of

Parameter	Value	Parameter	Value
m_1	0.8Kg	l_1	100mm
m_2	1.3Kg	l_2	400mm
m_3	2.4Kg	l_3	400mm
m_4	3.15Kg	l_4	100mm
m_5	2.4Kg	l_5	400mm
m_6	1.3Kg	l_6	400mm
m_7	0.8Kg	l_7	100mm
l_w	200mm	l_{fl}	200mm
l_{fw}	80mm		

Table 1. "Dany Walker" Model Parameters

freedom. The motors are mounted in such a way that their movements modify the robot's position in the frontal and sagittal plane. In particular, Figure 1(a) shows the frontal plane of the robot including the motors that control its movement, while the Figure 1(b) shows the sagittal plane.

In Figure 1(a), the positive direction of the x-axis corresponds to the robot's forward movement, the positive direction of the y-axis corresponds to the robot's movement to its left, and the positive direction of the z-axis is the opposite direction of gravity, while each mass is located in the middle of its corresponding link. The parameters of the robot model were set following the common standard as summarized in Table 1 and shown in Figure 3.

The foot length and width are 200 mm and 80 mm respectively. Let denote the position of the middle point of the supporting foot. And the robot motion is expressed with respect to the reference frame whose center is (x_s, y_s, z_s). Then the x-directional ZMP (x_{zmp}) and the y-directional ZMP (y_{zmp}) should be located in the following region:

$$\begin{array}{c} -100mm < x_{zmp} < 100mm \\ -40mm < y_{zmp} < 40mm \end{array} \quad (1)$$

If the ZMP falls within this region, thus it will belong to the convex hull of all contact points between the foot and the ground and therefore the biped robot can walk without falling down, see for instance Vukobratovic [73]. However, it is difficult to calculate the ZMP of a 3D robot model as in Figure 1(a) and 1(b) because of the coupling between the frontal plane (y-z plane) and sagittal plane (x-z plane) motions. The ZMP equations of the sagittal plane robot model and the frontal plane robot model are defined as follows

$$x_{zmp} = \frac{\sum_{i=1}^{7} m_i(\ddot{z}_i + g)x_i - \sum_{i=1}^{7} m_i\ddot{x}_i z_i}{\sum_{i=1}^{7} m_i(\ddot{z}_i + g)} \quad (2)$$

$$y_{zmp} = \frac{\sum_{i=1}^{7} m_i(\ddot{z}_i + g)y_i - \sum_{i=1}^{7} m_i\ddot{y}_i z_i}{\sum_{i=1}^{7} m_i(\ddot{z}_i + g)} \quad (3)$$

where g is gravity, and m_i are the position and mass of the $i-th$ point mass ($i = 1, ..., 7$), respectively as in Zlajpah [00].

3. WALKING TRAJECTORY ALGORITHM

The position of the robot is controlled in the frontal plane by means of driving the motors M1, M6, M5 and M10 (See Figure 1(a)). The walk sequence of a biped robot can be determined by controlling the hip and swing foot trajectories in the sagittal and frontal plane as studied in Takanishi [85] and Hiria [98]. In this case, we manipulate the motors M7, M8 and M9 for the left leg and M1, M2 and M3 for the right leg. This work shows how the robots stability was achieved by applying the ZMP criteria, while Hermite spline interpolation was used to generate the walking sequence.

3.1 Hermite spline interpolation

The cubic polynomials offer a reasonable balance between interpolation smoothness and computation speed. If it is compared to polynomials of higher degree, the cubic splines, require less calculations and smaller storage spaces, besides they are more stable.

A Hermite spline is a cubic polynomial interpolation in segments with adjustable derivatives at each control point. Opposite to the natural cubic splines, the Hermitian allows to define the segment locally, because each part of the curve only depends on the conditions of its extreme points. This is an important property for the generation of robot's trajectories, since it allows diminishing the speed while arriving to the final point, reducing the characteristic impact on the leg as soon as it establishes ground contact.

3.2 Trajectory generation

A walking motion can be considered as a repetition of one-step motion carried out in a period T_s. This step begins when the foot in movement leaves the floor and lift on the air and finishes when it returns to the floor. The double support phase begins when the foot in movement (at single support phase) touches the floor and ends when the foot at the floor (at single support phase) leaves the floor. To achieve dynamic walking, the change between simple supports phase and double supports phase should be executes smoothly. The walk sequence of a biped robot can be determined by controlling the hip and swing foot trajectories in the sagittal and frontal plane. Knowing the hip and swing foot movements, it is easy to solve the inverse kinematics problem for generating joint trajectories from the walking motion in Cartesian space.

3.3 Hip trajectory in the sagittal plane

The hip trajectory can be generated by Hermite spline polynomial algorithm, if the initial and final states are known from the single phase. Figure 2(b) shows the initial state as defined by $[x_{hs}, z_{hs}]$ and the final state by $[x_{he}, z_{he}]$. The initial velocity $[v_{xhs}, v_{zhs}]$ (produced when the robot leaves the initial position) is also specified in the trajectory model. The same case is for the final velocity $[v_{xhe}, v_{zhe}]$ (when the robot arrives to his final position).

The initial and final state positions for the cubic trajectory in z (the $z_h(t$ direction) can be expressed as follows:

$$z_h(t) = \begin{bmatrix} z_{hs} & if \quad t = kT \\ z_{he} & if \quad t = kT + T_s \end{bmatrix} \quad (4)$$

with T being the period for the robot's step and T_s the period in single support phase. It also yields

$$z_h(t) = \begin{bmatrix} v_{zhs} & if \quad t = kT \\ v_{zhe} & if \quad t = kT + T_s \end{bmatrix} \quad (5)$$

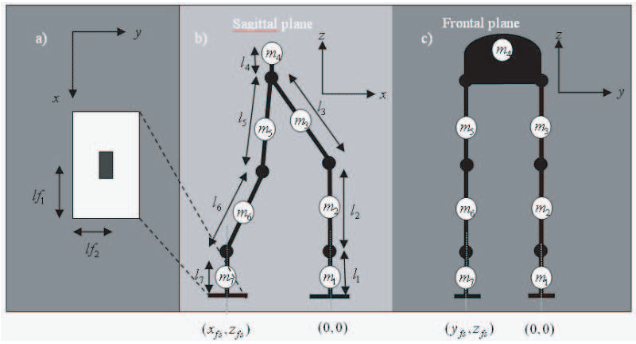

(a)

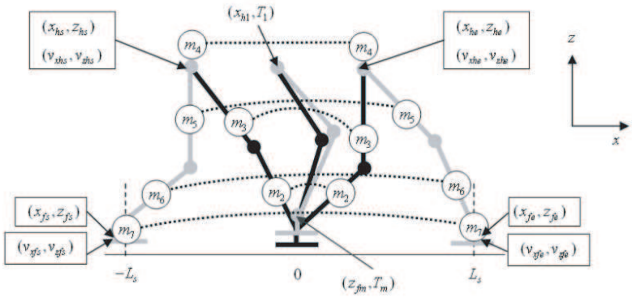

(b)

Fig. 2. "Dany Walker" notation: (a): Frontal plane. (b): Hip and swing foot trajectories in the sagittal plane

The cubic polynomial can be generalized by the following expression:

$$z_h(t) = a_0 + a_1 t + a_2 t^2 + a_3 t^3 \tag{6}$$

yielding

$$\begin{aligned} z_h(t) &= z_{hs} + v_{zhs}(t + kT) + \ldots \\ &\frac{3(z_{he} - z_{hs}) - 2v_{zhs}T_s - v_{zhe}T_s}{T_s^2} \ldots \\ &\frac{2(z_{hs} - z_{he}) + (v_{zhs} + v_{zhe})T_s}{T_s^3}(t - kT)^3 \\ &kT \leq t \leq kT + T_s \end{aligned} \tag{7}$$

$x_h(t)$ is divided into two parts: from $x_h(KT)$ to $x_h(kT + T1)$ and from $x_h(kT + T1)$ to $x_h(kT + Tp)$. The definition for $x_h(t)$ is shown by Equation 8 as follows:

$$\begin{cases} x_h(t) = x_{hs} & t = kT \\ x_h(t) = x_{h1} & t = kT + T_1 \\ x_h(t) = x_{hs} & t = kT + T_s \\ \dot{x}_h(t) = v_{xhs} & t = kT \\ \dot{x}_h(t^-) = x_h(t^+) & t = kT + T_1 \\ \dot{x}_h(t) = v_{xhe} & t = kT + T_s \\ \ddot{x}_h(t) = a_0 & t = kT \end{cases} \tag{8}$$

with a_o being previously specified to satisfy the initial condition of acceleration. The cubic polynomial trajectory can be calculated using Equation 9.

$$x_h(t) = \begin{cases} x_{hs} + v_{xhs}(t - kT) + \frac{1}{2}a_0(t - kT)^2 + \ldots \\ \frac{(x_{hl} - x_{hs} - v_{xhs}T_1 - \frac{1}{2}a_0T_1^2)(t - kT)^3}{T_1^3} \ldots \\ \qquad kT < t \leq kT + T_1 \\ \\ x_{h1} + v_{xh1}(t - kT - T_1) + \ldots \\ \frac{(3(x_{he} - x_{h1}) - 2v_{xh1}(T_p - T_1))(t - kT - T_1)^2}{(T_p - T_1)^2} + \ldots \\ \frac{(2(x_{h1} - x_{he}) - (v_{xh1} + v_{x2})(T_p - T_1))(t - kT - T_1)^3}{(T_p - T_1)^3} \\ \qquad kT + T_1 < t \leq kT + T_s \end{cases} \tag{9}$$

3.4 Swing foot trajectory in the sagittal plane

The Hermite spline polynomial interpolation is used to generate the foot trajectory in single support phase. In our case, in order to assure a smooth transition, the velocity (v_{xhs}, v_{zhs}) and (v_{xfe}, v_{zfe}) should be zero. The initial and final foot position (see Figure 2(b)) which represents the satisfied states and velocities can be obtained from:

$$x_f(t) = \begin{cases} x_f(t) = x_{fs} & t = kT \\ x_f(t) = x_{fe} & t = kT + T_s \\ \dot{x}_f(t) = 0 & t = kT \\ \dot{x}_f(t) = 0 & t = kT + T_s \end{cases} \tag{10}$$

$$z_f(t) = \begin{cases} z_f(t) = z_{fs} & t = kT \\ z_f(t) = z_{fe} & t = kT + T_s \\ \dot{z}_f(t) = 0 & t = kT \\ \dot{z}_f(t) = 0 & t = kT + T_s \end{cases} \tag{11}$$

From the initial and final states in x and z axis, a smooth trajectory can be generated by the Hermite spline interpolation yielding for $x_f(t)$=

$$x_{fs} + 3(x_{fe} - x_{fs})\frac{(t - kT)^2}{T_s^2} - 2(x_{fe} - x_{fs})\frac{(t - kT)^3}{T_s^3} \quad kT < t \leq kT + T_s \tag{12}$$

and for $z_f(t)$=

$$\begin{bmatrix} z_{fs} + 3(z_{fm} - z_{fs})\frac{(t - kT)^2}{T_m^2} - 2(z_{fm} - z_{fs})\frac{(t - kT)^3}{T_m^3} \\ kT < t \leq kT + T_m \\ and: \\ z_{fm} + 3(z_{fe} - z_{fm})\frac{(t - kT - T_m)^2}{(T_s - T_m)^2} - \ldots \\ 2(z_{fe} - z_{fm})\frac{(t - kT - T_m)^3}{(T_s - T_m)^3} \\ kT + T_m < t \leq kT + T_s \end{bmatrix} \tag{13}$$

The hip and knee position to produce the leg's movement can be calculated using the inverse kinematics of the robot's structure.

3.5 Hip trajectory in the frontal plane

The hip trajectory can be generated by Hermite spline polynomial algorithm. However in the front plane the movement is carried out in a cycle (see Figure 3), in which the hip moves from the initial position y_{hs} with an initial velocity v_{yhs} to the maximum allowed displacement y_{he}, all this within the half walking period $T_2 = T_s/2$. From that position y_{he} the hip moves again to its initial position y_{hs},

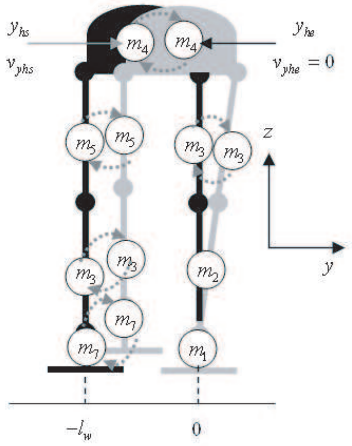

Fig. 3. Hip and swing foot trajectories in the frontal plane

executing a very smooth trajectory. It allows diminishing the speed while arriving to the final point, reducing the characteristic impact on the leg as soon as it establishes ground contact.

From the initial and final states in y, a smooth trajectory can be generated by the Hermite spline interpolation yielding for $kT < t \leq T_2$:

$$For \;\; kT < t \leq T_2$$

$$\begin{aligned} y_h(t) &= \\ y_{hs} &+ v_{yhs}(t-kT) + \frac{3(y_{he}-y_{hs}) - 2y_{yhs}T_2}{T_2^2}(t-kT)^2 + \\ &\ldots \frac{2(y_{hs}-y_{he}) - v_{yhs}T_2}{T_2^3}(t-kT)^3 \end{aligned} \tag{14}$$

$$For \;\; T_2 < t \leq T_s$$

$$\begin{aligned} y_h(t) &= \\ y_{he} &+ \frac{3(y_{hs}-y_{he})}{(T_s-T_2)^2}(t-kT)^2 - \frac{2(y_{hs}-y_{he})}{(T_s-T_2)^3}(t-kT)^3 \end{aligned}$$

3.6 Determination of the algorithm parameters

The determination of the parameters v_{xh}, T_1, T_m, z_{fm} and v_{yhs} is important because the modification of one of them supposes a change in the trajectory and conditions of smoothness in the velocity and accelerations. One of the most important features of this approach is that the linkage speed at the end of single support phase is zero or close to zero, therefore a smooth contact with the floor surface is guaranteed. If $T_1 = T_m = T_v$ then we have a single variable T_v that can be modified. If we calibrate T_v close to $T_s/2$, it yields a correct walking trajectory that guarantees the ZMP criterion. The trajectory smoothness allows avoiding the disturbances due to not modelled dynamics in motors.

4. WALKING MOTIONS

Figures 4(a), 4(b) and 4(c) show the walking motion using parameters from Table 1, and position trajectories (x_i, y_i, z_i) of the point masses (m_i), with a step period of $T_s = 2$sec and a step length of $L_s = 50$cm. Considering the equations 2 and 3, it is possible to separate the numerator, in such a way that it yields:

$$\begin{aligned} \sum_{i=1}^{7} m_i(\ddot{z}_i + g)x_i - \sum_{i=1}^{7} m_i\ddot{x}_i z_i &= \\ \ldots \sum_{i=1}^{7} m_i\ddot{z}_i x_i + \sum_{i=1}^{7} m_i g x_i - \sum_{i=1}^{7} m_i\ddot{x}_i z_i & \end{aligned} \tag{15}$$

for the axis x case. Therefore it could be defined that:

$$\begin{aligned} F1x &= \sum_{i=1}^{7} m_i\ddot{z}_i z_i & F1y &= \sum_{i=1}^{7} m_i\ddot{y}_i z_i \\ F2x &= \sum_{i=1}^{7} m_i g x_i & F2y &= \sum_{i=1}^{7} m_i g y_i \\ F3x &= \sum_{i=1}^{7} m_i\ddot{z}_i x_i & F3y &= \sum_{i=1}^{7} m_i\ddot{z}_i y_i \end{aligned} \tag{16}$$

Figures 5(a) and 5(b) show the trajectories of the moments defined in Equation 16. The ZMP trajectory shown in Figure 4(d) demonstrates that the ZMP is always kept in the foot support area using PTA.

Also, in order to demonstrate the influence of the smooth dynamic interaction between the feet and the ground produced for PTA, we have shown the step motion under the assumption that the contact between the swing foot and the ground is carried out over an uneven terrain. Under these conditions, pieces of materials were placed to 75 cm of the biped robot, giving as results the graph shown in Figures 6(a) and 6(b). The ZMP trajectory shown demonstrates that the ZMP is always kept in the foot support area using PTA, despite the surface disturbances.

In order to compare the robustness of the generated trajectories by TPA over irregular terrain, we use the approach IPM (see Zlajpah [00]) under the same conditions. Figure 6(b) shows such trajectories and the breaking point when the biped would fall as the ZMP went outside the support area. In fact only the robot is able to make two steps, after the terrain change. The TPA algorithm was programmed using Visual C++ and was tested on the “Dany Walker” biped robot, which was designed at the Freie Universitt Berlin.

5. CONCLUSION

In this paper, we proposed the TPA algorithm, which is simple and can reduce the ZMP error significantly in the trajectory generation of bipedal walking by simply smoothing the impact on the ground produced when the robot changes of walking phases. Based on some assumptions, we derived the equations used in TPA from the Hermite spline interpolation. We showed that these trajectories are well satisfied for bipedal walking motion. In order to see how TPA works, we generated the joint trajectories for walking motion, applied this walking motion to the 3D robot "Dany walker", and compared the results with the produced trajectories by IPM. The results showed that, the ZMP is always kept in the foot support area using PTA. We also studied the sensitivity of the ZMP trajectory produced by TPA and IPM in uneven terrain. These results showed that the ZMP is always kept in the foot support area using PTA; however in the IPM case the robot only was able to make two steps, after the terrain change.

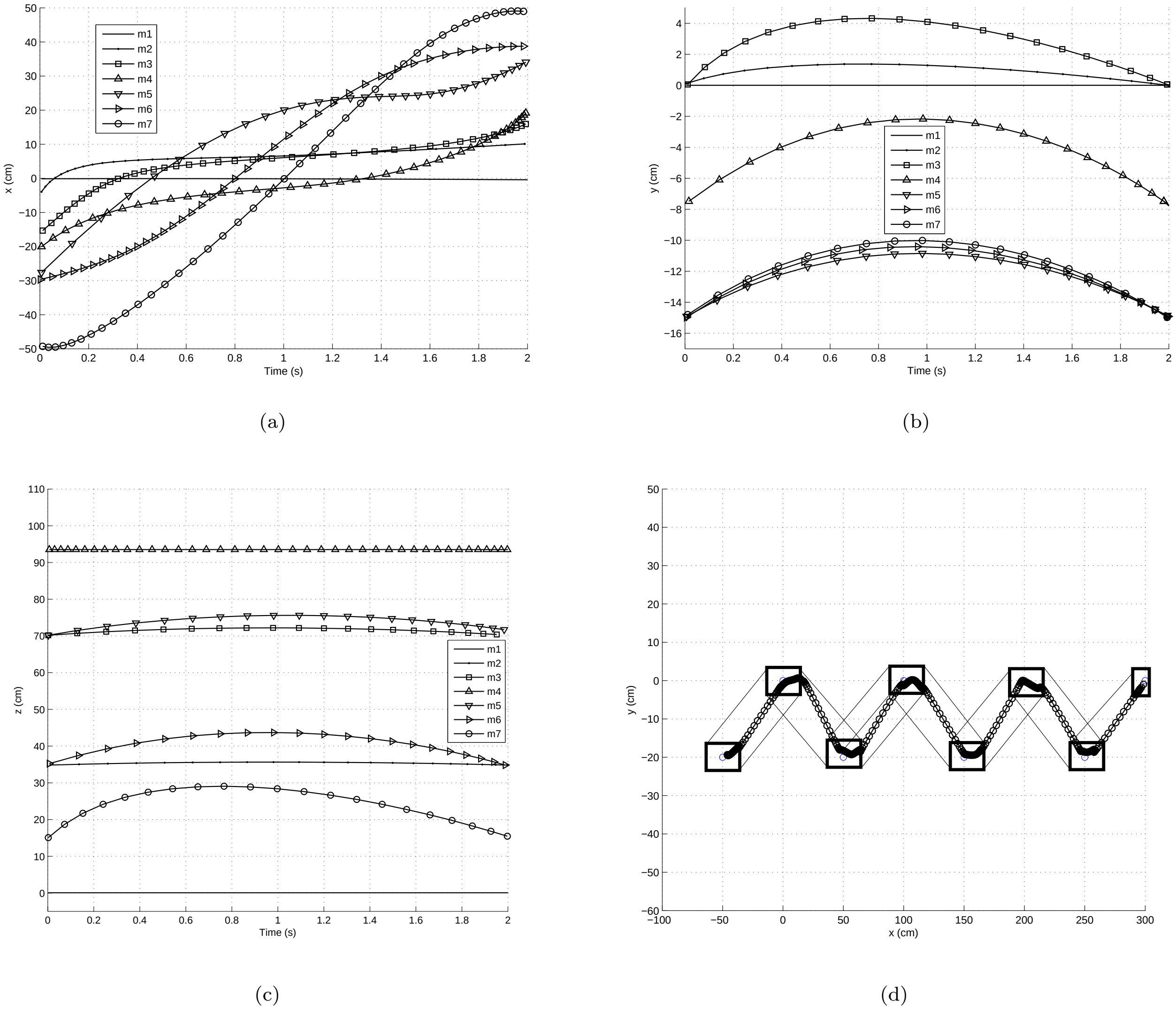

Fig. 4. Walking motions: (a): x trajectory, (b): y trajectory and (c): z trajectory, (d): ZMP trajectory using PTA.

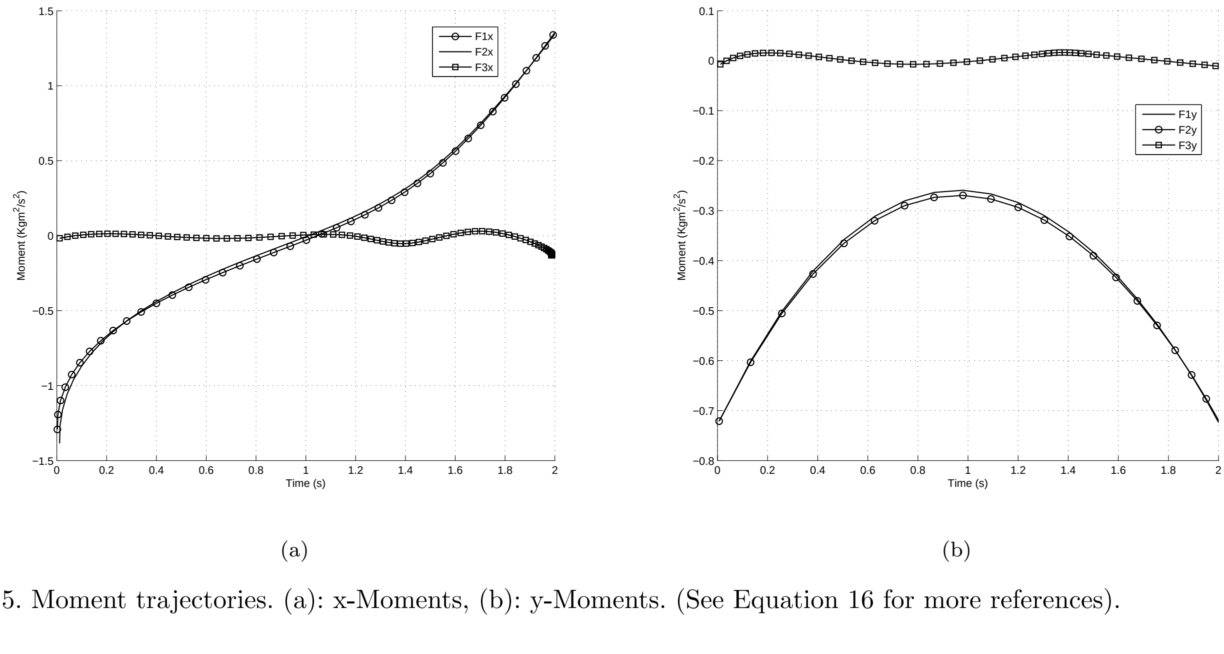

Fig. 5. Moment trajectories. (a): x-Moments, (b): y-Moments. (See Equation 16 for more references).

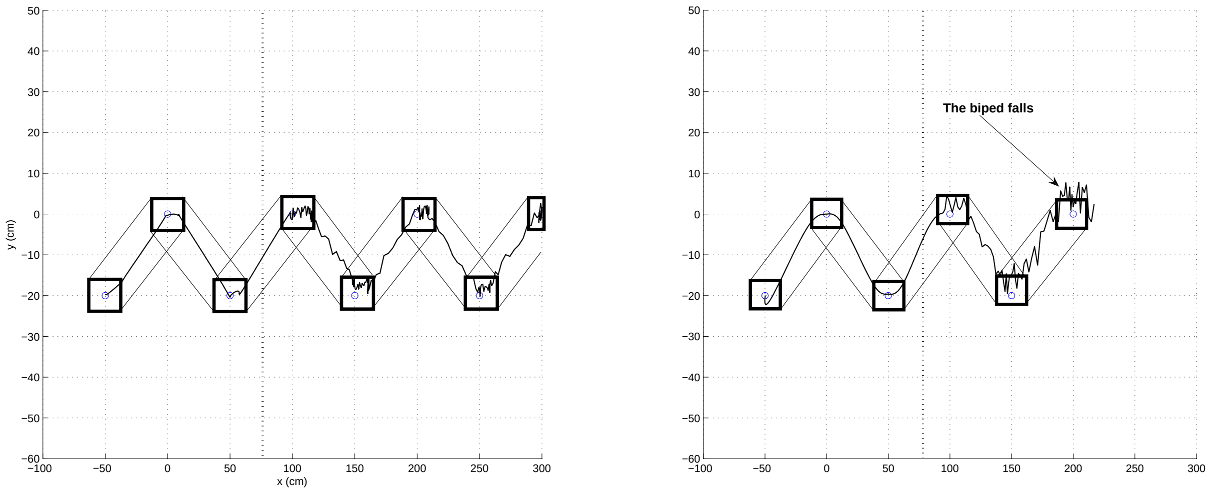

Fig. 6. ZMP trajectories over uneven terrains. (a) Results of the PTA Algorithm and (b) results of the IPM algorithm

REFERENCES

R. Goddard, Y. Zheng and H. Hemami Control of the heel-off to toe-off motion of a dynamic biped gait. *IEEE Trans. Syst. Man. Cyb.*, 22:1, 1992.

N. Kanehira, T. Kawasaki, S. Ohta, T. Isozumi, T. Kawada, F. Kanehiro, S. Kajita, K. Kaneko Design and experiments of advanced module (HRPL-2L) for humanoid robot (HRP-2) development. *Proc. 2002, IEEE-RSJ Int. Conf. Intell. Rob. Sys. EPFL, Lausanne, Switzerland*, volume 2, pages 2455–2460, 2002.

A. Konno, N. Kato, S. Shirata, T. Furuta and M. Uchiyama. *Development of a light-weight biped humanoid robot.* Proc. 2000 IEEE-RSJ Int. Con. Intell. Rob. Sys., 2000, 1565-1570

W. T. Miller III IEEE contr. Syst., vol. 14 *Real-time neural network control of a biped walking robot*, pages 41–48, 1994.

J. Yamaguchi, E. Soga, S. Inoue and A. Takanishi. *Development of a biped robot-control method of a whole body cooperative dynamic biped walking.* in Proc. 1999 IEEE Int. Conf. Robot. And Aut., Detroit, pages 368–374, 1999. Michigan.

G. Taga, Y. Yamaguchi and H. Shimizu Biol. Cyb., vol. 65 *Self-organized control of bipedal locomotion by neural oscilators in unpredictable environment*, pages 147–165, 1991.

S. Kajita, T. Yamaura and A. Kobayashi IEEE Trans. Robot and Automat., vol. 8 num. 4 *Dynamic walking control of a biped robot along a potiential energy conserving orbit*, pages 431–438, 1992.

Y. Zheng and J.Shen IEEE, Trans. Robot Automat., vol. 6 num. 1 *Gait synthesis for the SD-2 biped robot to climb sloped surface*, pages 86–96, 1990.

J. Pratt, C. M. Chew; A. Torres, P. D. and G. Pratt Int. Jo. Rob. Res., vol. 20 num. 2 *Virtual model control: an intuitive approach for bipedal locomotion*, pages 129–143, 2001.

S. Kajita and K. Tani IEEE Cont. Sys., vol. 16 num. 1 *Experimental study of biped dynamic walking*, pages 13–19, 1996.

C. L. Shih, Y. Z. Li, S. Churng, T. T. Lee and W. A. Cruver in Proc. 1990 IEEE Int. Conf. Rob. And Autom., *Trajectory synthesis and physical admissibility for a biped robot during the single support phase*, pages 1642–1652, 1990.

Q. Huang , K. Yokoi, S. Kajita, K. Kaneko, H. Arai, N. Koyachi and K. Tanie IEEE Trans. Rob. Aut., vol. 17 num. 6 *Planning walking patterns for a biped robot*, 1998.

Erik V. Cuevas, Daniel Zaldvar, and Ral Rojas Technical Report B-03-19, Freie Universitt Berlin, Fachbereich Mathematik und Informatik, Berlin, Germany *Bipedal robot description*, 2004.

M. Vukobratovic and D. Juricic IEEE Trans. Bio-Med. Eng., vol. BME-16 num. 1 *Contribution to the synthesis of biped gait*, pages 1–6, 1969.

M. Vukobratovic IEEE Trans. Syst. Man. Cyb., vol. SMC-3 num. 5 *How to control artificial anthropomorphic system*, pages 497–507, 1973.

A. Takanishi, M. Ishida, Y. Yamazaki and I. Kato in Proc. 1985, Int. Conf. Advanced Robotics, vol. 17 num. 6 *The realization of dynamic walking robot WL-10RD*, pages 459–466, 1985.

K. Hiria, M Hirose, Y. Haikawa, and T.Takenaka IEEE Int. Conf. Rob. and Aut., *The development of Honda Humanoid robot*, pages 1321–1332, 1998.

L. Zlajpah Jozef Stefan Institute, *Planar manipulators toolbox for use with MATLAB/SIMULINK.*

Albert Amos and Gerth Wilfried Journal of Intelligent and Robotic Systems, vol. 36 *Analytic path planning algorithms for bipedal robots without a trunk*, pages 109–127, 2004.

Taesi Ha, Chong-Ho Choi Robotic and Autonomus Systems, vol. 55 *An effective trajectory generation method for bipedal walking*, pages 795–810, 2007.